Characterization of MgSO$_4$ Hydrate for Thermochemical Seasonal Heat Storage

V. M. van Essen[1]
e-mail: v.vanessen@ecn.nl

H. A. Zondag

J. Cot Gores

L. P. J. Bleijendaal

M. Bakker

R. Schuitema

W. G. J. van Helden

Efficiency and Infrastructure,
Energy Research Centre of The Netherlands
(ECN),
P.O. Box 1,
1755 ZG Petten, The Netherlands

Z. He[2]

C. C. M. Rindt

Department of Mechanical Engineering,
Eindhoven University of Technology (TU/e),
5600 MB Eindhoven, The Netherlands

Water vapor sorption in salt hydrates is one of the most promising means for compact, low loss, and long-term storage of solar heat in the built environment. One of the most interesting salt hydrates for compact seasonal heat storage is magnesium sulfate heptahydrate (MgSO$_4$·7H$_2$O). This paper describes the characterization of MgSO$_4$·7H$_2$O to examine its suitability for application in a seasonal heat storage system for the built environment. Both charging (dehydration) and discharging (hydration) behaviors of the material were studied using thermogravimetric differential scanning calorimetry, X-ray diffraction, particle distribution measurements, and scanning electron microscope. The experimental results show that MgSO$_4$·7H$_2$O can be dehydrated at temperatures below 150°C, which can be reached by a medium temperature (vacuum tube) collector. Additionally, the material was able to store 2.2 GJ/m^3, almost nine times more energy than can be stored in water as sensible heat. On the other hand, the experimental results indicate that the release of the stored heat is more difficult. The amount of water taken up and the energy released by the material turned out to be strongly dependent on the water vapor pressure, temperature, and the total system pressure. The results of this study indicate that the application of MgSO$_4$·7H$_2$O at atmospheric pressure is problematic for a heat storage system where heat is released above 40°C using a water vapor pressure of 1.3 kPa. However, first experiments performed in a closed system at low pressure indicate that a small amount of heat can be released at 50°C and a water vapor pressure of 1.3 kPa. If a heat storage system has to operate at atmospheric pressure, then the application of MgSO$_4$·7H$_2$O for seasonal heat storage is possible for space heating operating at 25°C and a water vapor pressure of 2.1 kPa. [DOI: 10.1115/1.4000275]

Keywords: building, chemistry, heating, measurement, solar, storage, testing

1 Introduction

Households in The Netherlands use on average 65% of their energy consumption for space heating and domestic hot water. The energy consumption in the built environment can be reduced by energy saving measures (improved insulation, heat recovery, etc.). A substantial part of the remaining energy demand can be fulfilled by using renewable energy sources such as solar energy.

During summer, the heat demand can be completely covered using solar heat, but in winter the heat demand exceeds the solar supply. To accommodate this lag between the solar energy surplus in summer and the energy demand in winter, a seasonal thermal storage is needed.

Traditionally, water is used for storing solar heat (for example, solar boiler) for short time periods. However, water-based long-term heat storage will require a large tank (>50 m^3) that is often too large to be placed inside a building. As an alternative, it is possible to store energy by means of chemical processes, making use of the reversible reactions C+heat⇔A+B.

In the charging mode during summer, solid C dissociates under the influence of solar heat into components A and B, which are stored separately. In the discharging mode during winter, the two components (A and B) react to form solid C while releasing the stored solar heat. No reactions occur as long as the two components A and B are stored separately. Preliminary calculations show

that sensible heat losses comprise approximately 10% of the total energy storage; this means that the remaining energy can be stored loss-free.

A previous theoretical study [1] identified magnesium sulfate heptahydrate (MgSO$_4$·7H$_2$O) as a promising thermochemical material (TCM) for long-term heat storage, by means of the following reaction:

$$\text{MgSO}_4(\text{s}) + 7\text{H}_2\text{O}(\text{g}) \leftrightarrow \text{MgSO}_4 \cdot 7\text{H}_2\text{O}(\text{s}) + \text{heat} \qquad (1)$$

The theoretical storage density of MgSO$_4$·7H$_2$O is 2.8 GJ/m^3 [1], which offers a more compact way of storing energy for the same volume in comparison to water (0.25 GJ/m^3 in the temperature range 25–85°C). Additionally, MgSO$_4$·7H$_2$O is cheap, nontoxic, and noncorrosive. For these reasons, MgSO$_4$·7H$_2$O was studied as a possible TCM for solar seasonal heat storage within the Dutch WAELS project (Woningen Als Energie Leverend Systeem; House As Energy Supplying System).

The starting point of the investigation was that the material should be able to store and release solar heat under practical conditions. The TCM heat storage system is designed for a low-energy house with a heating demand of approximately 6 GJ for space heating and 9 GJ for domestic hot water preparation [2]. During summer a medium temperature collector (vacuum tube) is used to dehydrate the salt hydrate. It is assumed that these collectors deliver heat at a maximum temperature of 150°C. During winter, the water vapor is supplied by an evaporator/condenser connected to a borehole heat exchanger at 10°C. This means that a (saturation) water vapor pressure at 10°C [$P_{\text{H}_2\text{O}}^{\text{sat}}(10°\text{C})$ =1.3 kPa] is available during hydration in winter. In this paper, measurements are presented, which will give information on whether magnesium sulfate heptahydrate can be dehydrated using

---

a medium temperature collector and whether the dehydrated material is able to release the stored solar heat under practical conditions.

2 Experimental Method

2.1 Materials. Reagent grade magnesium sulfate heptahydrate (VWR BDH Prolabo, CAS 10034-99-8, NORMAPUR, 99.5% pure) was used in this work. The material was sieved prior to the experiments using a Fritsch vibratory shaker and sieves of 20 μm, 38 μm, 106 μm, 200 μm, and 500 μm to obtain powders with different particle size ranges. Unless stated otherwise, particles with a particle size distribution ranging from 38 μm to 106 μm were used during the experiments.

2.2 Thermal Analysis. Thermal analysis was used to obtain information on the dehydration and hydration behaviors of the material at atmospheric pressure (1 atm). Two thermal analysis techniques were used in this work: differential scanning calorimetry (DSC) and thermogravimetric (TG) analysis. TG analysis involves the measurement of the mass change as a function of temperature or time, and DSC involves the measurement of heat (enthalpy) changes as a function of temperature or time, in which both are subjected to a predefined temperature program (for more information on TG and DSC, see Ref. [3]).

The thermal analysis experiments described in this work were performed at the ECN (Petten, The Netherlands) and at Netzsch Application Laboratory (Selb, Germany). Both companies used a Netzsch STA 409 PC Luxx apparatus for investigation of the dehydration and hydration processes in the magnesium sulfate-water system, but the one at the ECN is equipped with a standard SiC furnace and the one at the Netzsch is equipped with a water vapor furnace especially built for performing humidity measurements. The Netzsch STA 409 PC Luxx apparatus can simultaneously perform TG and DSC measurements, also known as TG-DSC. A separate Netzsch DSC 204 F1 Phoenix apparatus at the ECN was used for a more accurate determination of the enthalpy of reaction.

Both hydration and dehydration measurements were performed by exposing the sample to a nitrogen-water vapor gas flow mixture. At the ECN, both STA 409 PC Luxx and DSC 204 F1 Phoenix apparatus used a mixture of dry and water vapor saturated nitrogen gas to achieve this nitrogen-water vapor atmosphere inside the machine. The mixture consisted of a nitrogen purge gas (60 ml/min), which was saturated with water vapor using a bubble flask at 20°C ($P_{H_2O}^{sat}=2.3$ kPa) and mixed inside the furnace with dry nitrogen protective gas with a flow rate of 20 ml/min. Since the STA apparatus at the ECN is not designed to handle moist gas flows, it was decided to keep the gas flows and bubble flask temperature fixed to protect the balance inside the machine. The humidity of the total gas mixture was measured at the exit of the Netzsch STA 409 PC Luxx apparatus using a dew point meter (Michell Optidew) and found to be ~40% at 25°C corresponding to a water vapor pressure of 1.3 kPa. The sample pans used during these experiments were made of aluminum oxide and were used without a lid. The sample masses ranged from 5 mg to 50 mg, where 10 mg was used as a standard sample mass.

To verify the experiments performed at the ECN, additional experiments were performed at the Netzsch Application Laboratory. The apparatus at the Netzsch was connected to a water vapor pressure control system, which allows performing experiments under moisturized nitrogen atmosphere with predefined relative humidity (accuracy of 1%). A nitrogen-water vapor gas mixture (30 ml/min) enters the sample chamber of the water vapor furnace of the STA. Due to the design of the furnace, it is prevented that the nitrogen protective gas flow (20 ml/min) arrives at the sample. As a result, humidity near the sample is not influenced by the protective gas and the relative humidity near the sample equals relative humidity from the water vapor pressure control system. The experiments were performed using platinum crucibles with pierced lids and a sample mass of ~10 mg. Nitrogen-water vapor atmospheres with $P_{H_2O}=1.3$ kPa at 25°C and $P_{H_2O}=2.1$ kPa at 30°C and 50°C were used during the experiments.

2.3 X-Ray Powder Diffraction. Information on the crystal structure of the different hydrates of magnesium sulfate before, during, and after dehydration and hydration was acquired using X-ray powder diffraction. The X-ray diffraction patterns were collected using a Bruker D8 Advance with a MRI oven with Cu KA1+KA2=1.5418 Å radiation. Typical runs were conducted with 2-theta ranging from 10 deg to 40 deg using a 0.05 deg 2-theta step with a time step of 2 s. The experimental diffraction patterns were compared with known patterns of magnesium sulfate hydrates [4]. Samples of 150 mg were placed on a platinum grid inside the oven and exposed to water vapor–nitrogen gas flow from a bubble flask at 22°C (corresponding to a saturation water vapor pressure of 2.7 kPa). The samples were dehydrated by increasing the temperature from 25°C to 300°C using a heating rate of 1°C/min. During hydration the temperature was held constant at 25°C. Diffraction patterns were recorded at temperatures where the TG curve indicated a change in composition.

2.4 Scanning Electron Microscopy. Microstructural changes on the grain level were observed using a JEOL JSM 6330F scanning electron microscope (SEM). The samples were placed on a carbon tape and mounted on a bronze stub. In order to improve the quality of the SEM picture, the samples were platinum coated by sputtering to enhance the conductivity of the material. The platinum coated samples were viewed under low-pressure 10^{-6}–10^{-7} mbar at magnifications ranging from $50\times$ to $1500\times$ in the SEM. The beam accelerator voltage was set between 5 kV and 15 kV.

2.5 Particle Size Distribution Measurements. The effect of hydration and dehydration on the particle size distribution was investigated using a Malvern Master 2000. This apparatus is capable of measuring materials in the range 0.02–2000 μm using the laser diffraction measurement principle (Mie scattering). During the laser diffraction measurements, a suspension of magnesium sulfate and ethanol is passed through a flow cell. Additionally, the suspension is shaken using ultrasound to prevent the magnesium sulfate particles from sticking together.

3 Results and Discussion

3.1 Dehydration Behavior of Magnesium Sulfate. The result of a TG-DSC experiment performed in a nitrogen-water vapor atmosphere with a heating rate of 1°C/min is shown in Fig. 1, and is typical for all dehydration measurements.

The quantitative data from the DSC measurements, literature values for reaction enthalpies, and calculated energy densities [1] are presented in Table 1.

The shape of the TG curve shows that the mass loss occurs in three steps, each accompanied by a change in DSC signal.

The first step occurs at a low temperature (25–55°C) involving a mass loss of $6.9 \pm 0.2\%$, which corresponds to the loss of one water molecule. The negative DSC peak shows that the first dehydration step is an endothermic process indicating that (solar) heat can be stored using this reaction. However, the fact that this transition of $MgSO_4 \cdot 7H_2O$ to $MgSO_4 \cdot 6H_2O$ already starts at 25°C means that when $MgSO_4 \cdot 7H_2O$ is stored under these conditions, it will (slowly) convert to $MgSO_4 \cdot 6H_2O$. As a result, less $MgSO_4 \cdot 7H_2O$ is available in the heat storage system and the amount of solar heat that can be stored using the first dehydration step decreases in time. This can also be seen in Table 1, where the value for the experimental reaction enthalpy is 19.3% lower than the theoretical value, probably due to partial conversion of $MgSO_4 \cdot 7H_2O$ to $MgSO_4 \cdot 6H_2O$ prior to the experiments.

Between the first and the second step, a melting process occurs at 52.5°C. This process can be identified by an additional DSC
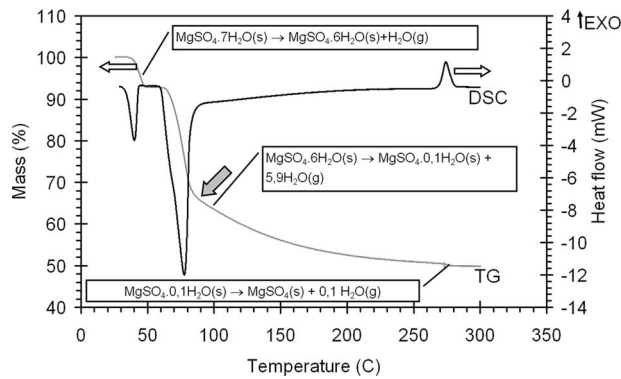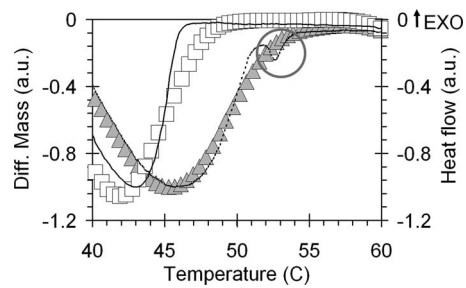
Fig. 1 Mass (TG) and heat flow (DSC) as a function of temperature for dehydration of $MgSO_4 \cdot 7H_2O$ with a particle size distribution of $38-106$ μm. The dehydration was performed by heating a sample of 10 mg from 25°C to 300°C with 1°C/min in a $N_2 + H_2O$ atmosphere assuming a $P_{H_2O} = 2.3$ kPa (see text for details). The gray filled arrow indicates the inflection point of the change in shape of the TG curve at the second dehydration step. Exothermic processes are indicated by a positive heat flow.

Fig. 2 Differential mass and heat flow as a function of temperature for particles with particle distributions of $200-500$ μm and $20-38$ μm. The measurements were performed by heating a sample of 10 mg from 25°C to 300°C with 1°C/min in a $N_2 + H_2O$ atmosphere assuming a $P_{H_2O} = 2.3$ kPa (see text for details). The open squares denote differential mass for $20-38$ μm particles, and the filled triangles $200-500$ μm particles. The lines denote the heat flow: solid line for $20-38$ μm particles and dashed line for $200-500$ μm particles. The circle indicates the peak associated with the observed melting process.

peak without an accompanying mass change as illustrated in Fig. 2.

The experimentally determined melting temperature of 52.5°C is in good agreement with the value of 50°C determined by Emons et al. [7] for the melting temperature of $MgSO_4 \cdot 7H_2O$. The fact that $MgSO_4 \cdot 7H_2O$ melts during dehydration can be an additional problem for the application of the first dehydration step for storage of solar heat: Melting reduces the bed porosity of the material and thereby the vapor transport through the bed, limiting the ability of the material to take up the water again. As can be seen from Fig. 2, it seems that melting typically occurs for large particles and can be avoided when small particles are used. Further investigation using different heating rates (0.5°C/min, 1°C/min, and 5°C/min), different sample sizes (5 mg, 10 mg, 20 mg, and 50 mg), and different particle size distributions ($20-38$ μm, $38-106$ μm, $106-200$ μm, and $200-500$ μm) revealed that melting was not observed when low heating rates (≤ 1°C/min), small particles (<200 μm), and/or small sample sizes (≤ 5 mg) are being used. In a heat storage system, which will use large quantities of material, it will be very difficult to meet these criteria.

The second dehydration step in Fig. 1 occurs between 60°C and 265°C. From the shape of the TG curve, it can be seen that the second dehydration step consists of at least two dehydration steps: An initial steep decrease in weight loss signal is followed by a more gradual decrease (note the inflection point indicated by the gray arrow in Fig. 1). Interestingly, the sharp drop in mass

corresponds to a loss of approximately four water molecules. This suggests that the dehydration of $MgSO_4 \cdot 6H_2O$ proceeds through a $MgSO_4 \cdot 2H_2O$ intermediate. However, this could not be confirmed by other techniques such as X-ray diffraction (see also Fig. 3) under similar conditions. The total mass loss in the second step is $42.2 \pm 0.3\%$ corresponding to the loss of 5.9 water molecules. This means that the overall second dehydration step involves the transitions from $MgSO_4 \cdot 6H_2O$ to $MgSO_4 \cdot 0 \cdot 1H_2O$. The existence of $MgSO_4 \cdot 0 \cdot 1H_2O$ seems strange at first sight. However, under all conditions the TG curve for dehydration always showed a third mass loss at high temperatures (near 275°C), which indicates that there is still some water present in the material after the second dehydration step (see discussion below). The second dehydration step is accompanied by a negative DSC peak indicating that this transition is also endothermic. The value for the enthalpy of reaction ($\Delta_r H$), as shown in Table 1, is in good agreement with literature value from Wagman et al. [6]. Table 1 also shows that the energy density associated with the second dehydration step is the largest of the three dehydration steps: 2.2 GJ/m^3 (based on solid density of $MgSO_4 \cdot 7H_2O$), which means that nine times more energy can be stored using this dehydration step than can be stored in water as sensible heat (0.25 GJ/m^3 in the temperature range $25-85$°C). It should be noted that the sharp endothermic heat flow and the sharp drop in mass in Fig. 1 both end at $\sim 80-90$°C, which suggests that the first part of the second dehydration step (with possible formation of $MgSO_4 \cdot 2H_2O$ intermediate) can be used to store large amounts of energy. The DSC curve in Fig. 1 shows that almost no energy can be stored between 150°C and

Table 1 Experimental and theoretical enthalpies of reaction and energy densities for dehydration reactions of magnesium sulfate hydrates

Reaction	$\Delta_r H$ (kJ/mol)			Energy density (GJ/m^3) [a]	
	This study	Ref. [6]	Abs. diff. (%)	This study	Ref. [6]
$MgSO_4 \cdot 7H_2O(s) \rightarrow MgSO_4 \cdot 6H_2O(s) + H_2O(g)$	50.2	59.9	19.3	0.3	0.4
$MgSO_4 \cdot 6H_2O(s) \rightarrow MgSO_4 \cdot 0 \cdot 1H_2O(s) + 5 \cdot 9H_2O(g)$ [b]	318.9	340.7	6.8	2.2	2.3
$MgSO_4 \cdot 0 \cdot 1H_2O(s) \rightarrow MgSO_4(s) + 0 \cdot 1H_2O(g)$	-15.1 [c]	6.1	140.3	-0.1	4.0×10^{-2}

[a] Energy densities were calculated from the enthalpy of reaction using the solid density of $MgSO_4 \cdot 7H_2O$ ($= 1.68$ g/cm^3 [5]).
[b] Theoretical enthalpy of formation for $MgSO_4 \cdot 0 \cdot 1H_2O$ of -1319.6 kJ/mol was found by fitting enthalpies of formation for hydrates of magnesium sulfate from Wagman et al. [6] as a function of the amount of hydrated water molecules.
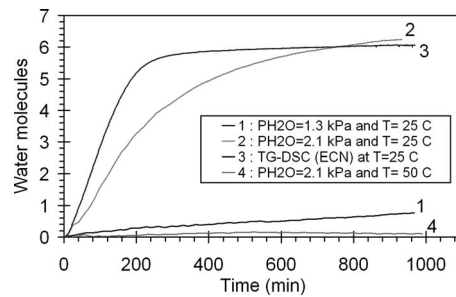[c] The DSC peak also includes a recrystallization process.
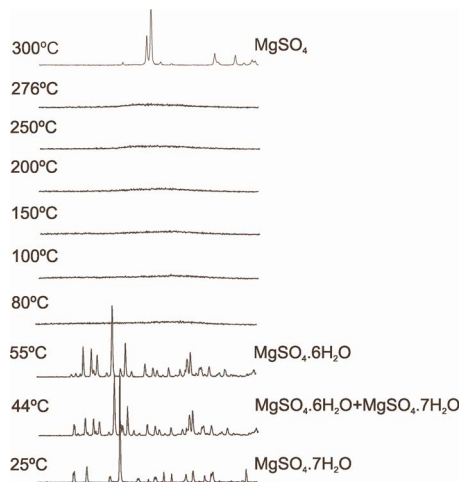
Fig. 3 X-ray diffraction patterns taken at different temperatures during the dehydration of $MgSO_4 \cdot 7H_2O$. The same particle size distribution (38–106 μm) and identical temperature program as described in Fig. 1 were used during the dehydration of $MgSO_4 \cdot 7H_2O$ as described.

Fig. 4 Number of water molecules taken up in a hydration experiment of $MgSO_4$ as a function of time. The results from the Netzsch (curves 1, 2, and 4) and the results from the ECN (curve 3) are shown. In all cases, a sample of 10 mg was dehydrated from 25°C to 300°C with 1°C/min. After 15 min isothermally at 300°C, the samples were cooled down to 25°C or 50°C with 5°C/min and exposed to a moist nitrogen atmosphere as indicated in the figure. During the experiments a particle size distribution of 38–106 μm was used.

265°C using the second dehydration step. It means that approximately 2.2 GJ/m^3 can be stored when heating $MgSO_4 \cdot 6H_2O$ to 150°C using a medium temperature collector, which makes the second dehydration step very interesting for compact seasonal heat storage.

Finally, the third dehydration step in Fig. 1 takes place at a high temperature of 275°C and involves the mass loss of $0.5 \pm 0.1\%$ corresponding to 0.1 water molecules. It means that during the last dehydration step $MgSO_4 \cdot 0 \cdot 1H_2O$ is converted to anhydrous $MgSO_4$. Surprisingly, the corresponding DSC peak is positive indicating an exothermic process, which is in contrast to the previous two dehydration steps where the loss of water molecules was identified as an endothermic process. In fact, Table 1 shows that the theoretical value for the enthalpy of reaction is positive. Ruiz-Agudo et al. [8] also found that the final transition to $MgSO_4$ involves an exothermic process and suggests that this process is a result of a recrystallization from an amorphous precursor to crystalline $MgSO_4$. This suggestion was further investigated by means of X-ray diffraction. Figure 3 shows the experimental X-ray diffraction patterns obtained during the dehydration of $MgSO_4 \cdot 7H_2O$.

When the temperature of the sample is increased, the X-ray diffraction patterns show that $MgSO_4 \cdot 7H_2O$ is completely converted to $MgSO_4 \cdot 6H_2O$ at $T = 55°C$. This observation is in agreement with the result obtained by TG-DSC experiment (see above). The X-ray diffraction patterns for temperatures between 80°C and 276°C show that in this temperature range an amorphous phase is formed, which converts to crystalline $MgSO_4$ at 300°C. The recrystallization of the amorphous phase to crystalline $MgSO_4$, together with the exothermic process found at ~275°C in the DSC measurement (see Fig. 1), confirms the observation made by Ruiz-Agudo et al. [8] that the last dehydration step involves an exothermic recrystallization. Additionally, the X-ray diffraction pattern at 300°C confirms that the material is completely dehydrated at this temperature when using a heating rate of 1°C/min.

3.2 The Influence of Partial Water Vapor Pressure on the Hydration Behavior of $MgSO_4$ at 25°C and 1 atm. In a thermochemical heat storage system, the hydration reaction determines the amount of power delivered to the load and the temperature at which the power can be delivered. For this reason, it is essential to understand the hydration behavior of the material, so that the solar heat stored during dehydration can be fully released.

The hydration behavior of $MgSO_4$ was studied using thermal analysis by allowing the anhydrous material from the dehydration experiments (see above) to cool down from 300°C to 25°C with 5°C/min. Next, the sample was exposed for 16 h to a moist nitrogen atmosphere at atmospheric pressure with a constant partial water vapor pressure. The results of these measurements are presented in Fig. 4.

Initial experiments at the ECN (curve 3 in Fig. 4) were performed at 25°C while subjecting the anhydrous material to a partial water vapor pressure of 1.3 kPa (or RH=40% at 25°C). To check these results it was decided to repeat the measurement at the Netzsch under identical conditions. A remarkable difference was observed between the TG-DSC measurements under the same conditions performed at the Netzsch (curve 1 in Fig. 4) and at the ECN (curve 3 in Fig. 4): After 16 h, the result from the Netzsch indicates that the material takes up approximately one water molecule, while the result from the ECN indicates that $MgSO_4$ takes up six water molecules. The results in Fig. 4 show that at a higher water vapor pressure of 2.1 kPa, the result of the Netzsch (curve 2 in Fig. 4) is similar to the result acquired at the ECN. The experiments at the Netzsch were performed using a premixed nitrogen-water vapor gas flow with predetermined water vapor pressure (see above), while at the ECN a dry nitrogen gas flow was mixed with a water vapor saturated nitrogen gas flow ($P_{H_2O}^{sat}$=2.3 kPa at 20°C) inside the furnace. Possible incomplete mixing of these two gas flows during the experiments performed at the ECN may have resulted in a higher local partial water vapor pressure near the sample than the value determined at the exit of the apparatus. The exact value of the local water vapor pressure near the sample was not determined since it was assumed that gas flows were completely mixed near the sample. A closer look at the shape of the curves in Fig. 4 reveals that the water uptake during the experiments at the ECN (curve 3 in Fig. 4) is faster than the water uptake rate at the Netzsch (curve 2 in Fig. 4), suggesting an even higher water vapor pressure than 2.1 kPa. A possible explanation for this observation is that the sample is directly exposed to the water vapor saturated nitrogen purge gas flow with $P_{H_2O}^{sat}$ =2.3 kPa at 20°C (see above), and that mixing with the dry nitrogen protective gas flow only occurs downstream of the gas flow. For this reason, it is assumed in this paper that the partial water vapor pressure for the results from the ECN is 2.3 kPa instead of 1.3 kPa. However, more experiments are required to verify this. It is important to note that the result from the ECN shown in Fig. 4 was reproducible: The same water uptake was observed for $MgSO_4$ at 25°C and constant gas flows for all

Table 2 Overview of experimental hydration and dehydration enthalpies and energy storage densities

	Dehydration[a]	Hydration at 25°C and $P_{H_2O}=2.3$ kPa
Overall reaction	$MgSO_4 \cdot 6H_2O(s) \rightarrow$ $MgSO_4(s)+6H_2O(g)$	$MgSO_4(s)+6H_2O(g) \rightarrow$ $MgSO_4 \cdot 6H_2O(s)$
$\Delta_r H$ (kJ/mol)	303.8 ± 15.2	268.4 ± 13.4
$\Delta_r H$ (kJ/mol H_2O)	50.6 ± 2.5	44.7 ± 2.2
Energy density (GJ/m^3)	2.1 ± 0.1	1.8 ± 0.1

[a]Values were obtained by adding enthalpies and energy storage densities for the second and third dehydration steps 2 and 3 (see also Table 1).

samples and particle sizes discussed in the paper, which indicates a constant partial water vapor pressure near the sample.

Curves 2 and 3 in Fig. 4 show no inflection point (see, for example, the gray arrow in Fig. 1), which means that the transition from $MgSO_4$ to $MgSO_4 \cdot 6H_2O$ occurs as a single step without the formation of intermediates. This is confirmed by X-ray diffraction patterns where only the X-ray diffraction patterns for $MgSO_4$ and $MgSO_4 \cdot 6H_2O$ were observed.

The reaction enthalpy of the transition from $MgSO_4$ to $MgSO_4 \cdot 6H_2O$ was determined using a Netzsch DSC 204 F1 apparatus (see above). These experiments were performed under identical conditions as the TG-DSC experiments at the ECN. In Table 2 the enthalpy of hydration is compared with the enthalpy of dehydration, both determined in these separate DSC experiments.

The values for the enthalpy of hydration and dehydration are in good agreement (~88% of the stored energy is released at 25°C while exposed to a water vapor pressure of 2.3 kPa) indicating that the stored solar heat can be retrieved after one dehydration-hydration cycle. However, in a heat storage system, the material is exposed to a significant lower partial water vapor pressure (1.3 kPa instead of 2.3 kPa). As can be seen in Fig. 4, $MgSO_4$ takes up one water molecule during 16 h at 25°C and a partial water vapor pressure of 1.3 kPa. The enthalpy of hydration for this reaction could not be determined, but based on Table 2 only 15% (=44.7 kJ/mol instead of 303 kJ/mol) of the stored energy is released when one water molecule is taken up by the material.

3.3 Influence of Particle Size and Layer Thickness on Water Take Up at Constant Water Vapor Pressure, 25°C, and 1 atm. The effect of the particle size on hydration was investigated at the ECN using thermal analysis for four particle size distributions: 20−38 μm, 38−106 μm, 106−200 μm, and 200−500 μm. The material was thermally dehydrated prior to the hydration experiments as described above. The anhydrous material was cooled down from 300°C to 25°C with 5°C/min and subsequently exposed to a nitrogen-water vapor atmosphere with $P_{H_2O}=2.3$ kPa (see discussion above) during both dehydration and hydration. The effect of particle size distribution on hydration for a sample of 10 mg is presented in Fig. 5.

The results clearly show that the variation in the particle size distribution has a very limited effect on the hydration, since the water uptake for all studied particle size distributions corresponds to six water molecules. It means that the internal mass transfer resistance for the studied particle size distributions is not significant. Next, the effect of layer thickness on the hydration rate at 25°C was studied to investigate whether the mass transfer resistance between the particles can influence the water uptake. These experiments were performed using a constant particle size distribution of 38−106 μm. The samples were placed in crucibles with a constant volume of 72 mm^3. Since identical crucibles were used during each experiment, it was possible to alter the layer thickness by varying the sample mass. The experiments were performed for sample masses of 5 mg, 20 mg, and 50 mg, which correspond to layer thicknesses of 0.1 mm, 0.4 mm, and 1.1 mm, respectively.
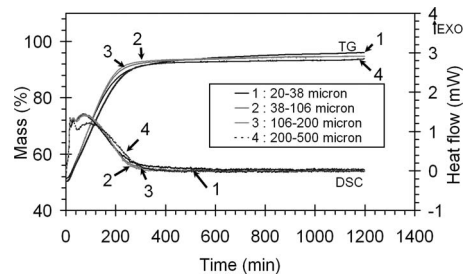
Fig. 5 Mass (TG) and heat flow (DSC) as a function of time for hydration of $MgSO_4$ at 25°C and $P_{H_2O}=2.3$ kPa for four different particle distributions. In all cases a sample mass of 10 mg was used.

As can be seen from the results presented in Fig. 6, the hydration is strongly affected by a change in layer thickness: For smaller layer thickness, the reaction is completed in a shorter time. Since an increase in layer thickness results in a slower hydration rate, it indicates that the vapor transport through the layer is a limiting factor in the hydration process.

3.4 The Effect of Dehydration and Hydration at 25°C and 1 atm on Grains. Ruiz-Agudo et al. [8] investigated the morphology of a $MgSO_4 \cdot 7H_2O$ crystal and observed that during the dehydration of $MgSO_4 \cdot 7H_2O$ cracks and pores were formed due to the release of water vapor, while the initial surface appeared to be smooth. This was further investigated by taking SEM images from grains before and after dehydration, and after hydration. The SEM images are shown Fig. 7.

Before dehydration of the material, small cracks are visible on a grain surface. Next, 40 g of material was heated up inside an oven from 20°C to 150°C with 1°C/min. The dehydration resulted in a mass loss of 42.2%, which corresponds to the formation of $MgSO_4 \cdot H_2O$. This result is in agreement with the mass loss found during the TG-DSC measurement at 150°C (see also Fig. 1). The SEM images of this material clearly show the formation of more cracks and pores. After dehydration, the material was hydrated for 20 h inside a climate room (ESPEC PL-3KPH) at 20°C and RH=52% corresponding to a water vapor pressure of 1.2 kPa. As can be seen from Fig. 7, it appeared that the number of cracks and pores was constant after the dehydrated material takes up water vapor. No further crack or pore formation was observed when the material was again subjected to a dehydration-hydration cycle (not shown in Fig. 7).

The particle size distributions of the material before and after dehydration, and after hydration are presented in Fig. 8.

The material was sieved to acquire particles of 38−106 μm prior to the experiments. The particle distribution before dehydration ("untreated" in Fig. 8) shows a good correspondence between the expected particle distribution based on sieving the material and the actual particle distribution. After dehydration, the particle
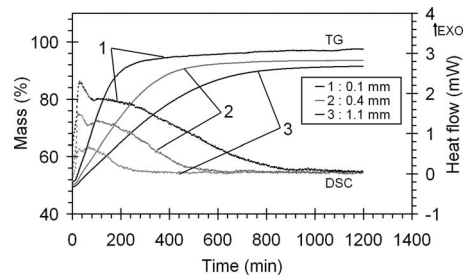
Fig. 6 Mass (TG) and heat flow (DSC) as a function of time for hydration of $MgSO_4$ at 25°C and $P_{H_2O}=2.3$ kPa for three different values for the layer thickness
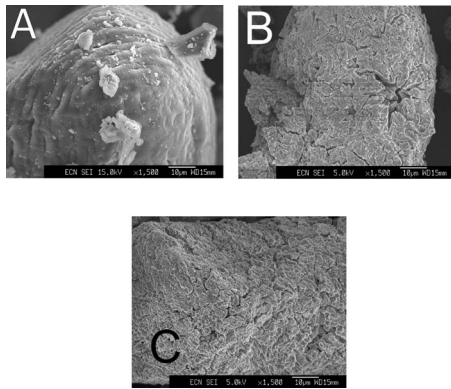
Fig. 7 SEM images of particles (38–106 μm): (a) before dehydration (15 kV, 1500× magnification), (b) after dehydration (5 kV, 1500× magnification), and (c) after hydration (5 kV, 1500× magnification). The material was dehydrated to 150°C with 1°C/min inside an oven and hydrated for 20 h inside a climate room (ESPEC PL-3KPH) at 20°C and RH=52%, corresponding to P_{H_2O}=1.2 kPa.

size is reduced and a fraction of small particles are formed ($\sim$1 –10 μm). Apparently, the formation of new cracks and pores is so violent that smaller particles are expelled during the dehydration. This can also be seen in the SEM images where holes in the grain are clearly visible after dehydration as shown in Fig. 7(b). The formation of small particles during dehydration can be a problem for a future TCM reactor; for example, when a fluidized bed is used, the smaller particles could flow out of the reactor before being (de)hydrated. The results in Fig. 8 show that when the dehydrated material takes up water, the particle size distribution is almost not affected: A small shift to larger particles is observed. The dehydration and hydration reactions result in a significant variation in molar volume between $MgSO_4 \cdot H_2O$ and $MgSO_4 \cdot 6H_2O$ (a factor of 2.5 based on the solid density). The results in Fig. 8 show a smaller change in particle size distribution, which is surprising when considering the large variation in molar volume. A possible explanation for this behavior is that the grain size remains constant but the porosity of the grain changes upon hydration and dehydration. However, more research is needed to fully understand this behavior.

3.5 Hydration of Magnesium Sulfate Under Practical Conditions. In our TCM heat storage system, the material is dehydrated and exposed to a partial water vapor pressure of 1.3 kPa (see above). The experimental results in Fig. 4 show that $MgSO_4$
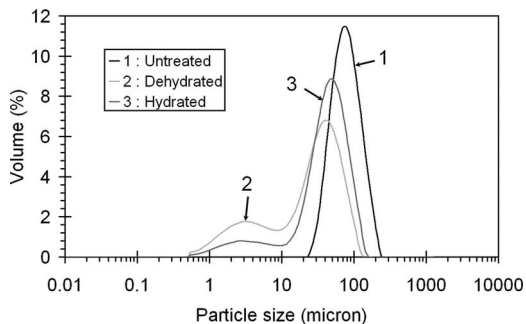
Fig. 8 Particle size distribution of $MgSO_4 \cdot 7H_2O$: before (curve 1, untreated) and after (curve 2) dehydration, and after hydration (curve 3). The material was dehydrated to 150°C with 1°C/min inside an oven and hydrated for 20 h inside a climate room (ESPEC PL-3KPH) at 20°C and RH=52%, corresponding to P_{H_2O}=1.2 kPa.
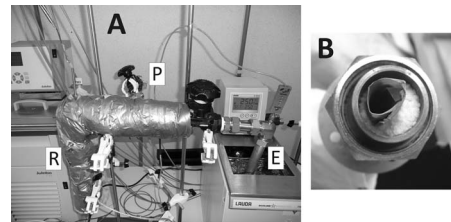
Fig. 9 (a) Fixed-bed reactor setup for testing the hydration behavior of magnesium sulfate under low-pressure conditions. R denotes the reactor, E denotes the evaporator, and P denotes connection to vacuum pump system, (b) Top view of fixed-bed reactor with metal mesh vapor channel.

takes up one water molecule at 25°C and P_{H_2O}=1.3 kPa. As mentioned before, under these conditions, only 15% of the stored heat is released. The released solar heat can be used for space heating, for example, for underfloor heating, which normally operates at temperatures $T \geq 40$°C. It means that the material should be able to hydrate and release heat at these temperatures and P_{H_2O}=1.3 kPa. For this reason, the water uptake of the anhydrous material was studied at 50°C using the STA apparatus at the Netzsch.

The hydration experiments at 25°C (see Fig. 4) showed that the largest amount of water was taken up by $MgSO_4$ when the partial water vapor pressure was 2.1 kPa. For this reason, it was decided to also use this water vapor pressure at 50°C to study the effect of temperature on hydration. The result of the hydration experiment performed at 50°C and P_{H_2O}=2.1 kPa is shown as curve 4 in Fig. 4. The effect of increasing the temperature from 25°C (curve 2 in Fig. 4) to 50°C at constant water vapor pressure of 2.1 kPa is evident: $MgSO_4$ is unable to take up water at 50°C. A similar observation was made by Chipera and Vaniman [9], who found that $MgSO_4$ converted to $MgSO_4 \cdot 6H_2O$ only at a very high water vapor pressure of 9.3 kPa (or RH=75% at 50°C). Since a partial water vapor pressure higher than 1.3 kPa cannot be achieved (see above), it means that the application of magnesium sulfate for compact seasonal heat storage at atmospheric pressure in our TCM heat storage system is quite problematic.
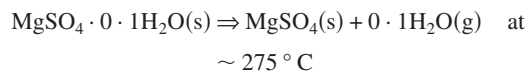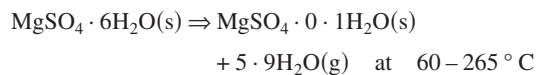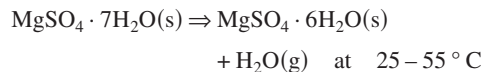
Another system type that is often used for (seasonal) heat storage is the closed system. These closed heat storage systems often operate under low pressure in order to facilitate the water vapor transport through a medium. A separate experiment was performed using a fixed-bed reactor to test the hydration behavior of magnesium sulfate at low pressure and under the aforementioned operating conditions. This experimental setup is shown in Fig. 9.

The fixed-bed reactor has a storage volume of 98 ml. A cylindrical metal mesh with an aperture size of 40 μm and a diameter of 1 cm is placed in the center of the reactor and acts as a vapor channel to facilitate the water transport to the salt (see Fig. 9(b)). Prior to the experiment, 25 g of $MgSO_4 \cdot 7H_2O$ was dehydrated at 150°C at atmospheric pressure inside an oven, which resulted in the transformation from $MgSO_4 \cdot 7H_2O$ to $MgSO_4 \cdot H_2O$. The reactor was filled with the dehydrated material from the oven. Next, the reactor was connected to the evaporator and a vacuum pump system consisting of two diaphragm vacuum pumps and a pressure sensor (not shown in Fig. 9). The evaporator is immersed in a thermostat bath to keep the temperature of the water inside the evaporator constant at 10°C ($P_{H_2O}^{sat}$=1.3 kPa). The system was evacuated to 2.8 mbar using the vacuum pump system in order to promote the diffusion of water vapor to the salt hydrate. During the hydration experiment, the reactor temperature was kept constant at 50°C by means of a heating cable located around the reactor. Thermocouples located inside the reactor monitored the temperature during the hydration. A maximum temperature increase of 4°C in the reactor was observed during the hydration, which indicates that under low-pressure magnesium sulfate reacts

with water vapor producing enough heat to create this small temperature lift. This result was unexpected, since the sample mass (and layer thickness) was larger than the samples used in the STA (5–50 mg). Therefore, it was expected that the vapor transport through the (thicker) layer would be so slow that a temperature lift could not be detected (see discussion above). Apparently, the low-pressure condition significantly improves the vapor transport through the layer. Although more detailed experiments are required to investigate this process and the actual amount of energy released, the results indicate that a closed system operating at reduced pressure is highly recommended for application of magnesium sulfate as thermochemical material for compact seasonal heat storage.

4 Summary and Conclusions

Magnesium sulfate heptahydrate ($MgSO_4 \cdot 7H_2O$) was investigated as potential TCM for compact seasonal heat storage. The results show that the dehydration of $MgSO_4 \cdot 7H_2O$ proceeds in at least three steps:

$$MgSO_4 \cdot 7H_2O(s) \Rightarrow MgSO_4 \cdot 6H_2O(s)$$
$$+ H_2O(g) \quad \text{at} \quad 25 - 55\,°C$$

$$MgSO_4 \cdot 6H_2O(s) \Rightarrow MgSO_4 \cdot 0 \cdot 1H_2O(s)$$
$$+ 5 \cdot 9H_2O(g) \quad \text{at} \quad 60 - 265\,°C$$

$$MgSO_4 \cdot 0 \cdot 1H_2O(s) \Rightarrow MgSO_4(s) + 0 \cdot 1H_2O(g) \quad \text{at}$$
$$\sim 275\,°C$$

The second dehydration step has a high-energy density (2.2 ± 0.1 GJ/m^3), the reaction primarily occurs in a temperature range that can be covered by medium temperature collectors ($\leq 150°C$), and problems with melting of the $MgSO_4 \cdot 7H_2O$ can be avoided. Therefore, this step is most interesting for compact seasonal solar heat storage.

Experiments indicate that the second dehydration step involves several consecutive dehydration steps, probably including a $MgSO_4 \cdot 2H_2O$ intermediate, but it was not possible to clearly identify each individual step. X-ray diffraction experiments indicated that the second dehydration step involves a material structure change from crystalline ($MgSO_4 \cdot 6H_2O$) to an amorphous phase until crystalline $MgSO_4$ is formed.

Hydration experiments performed at atmospheric pressure reveal that the amount of water taken up by $MgSO_4$ depends on partial water vapor pressure and the temperature. Experiments reveal that at 25 °C an increase in water vapor pressure from 1.3 kPa to 2.1 kPa results in improved water uptake: Six water molecules instead of one water molecule are taken up per $MgSO_4$ molecule. The single step transformation from $MgSO_4$ to $MgSO_4 \cdot 6H_2O$ has an energy density of 1.8 ± 0.1 GJ/m^3, which is approximately 88% of the energy density of the corresponding

dehydration reaction (2.1 ± 0.1 GJ/m^3). Increasing the temperature from 25 °C to 50 °C at constant $P_{H_2O} = 2.1$ kPa results in a strongly reduced water uptake by $MgSO_4$. It means that under practical conditions (partial water vapor pressure of 1.3 kPa and $T > 40°C$), the material is not able to take up water at atmospheric pressure. However, an initial test using a closed fixed-bed reactor operating at low pressure showed a maximum temperature increase of 4 °C. This result indicates that under low-pressure conditions dehydrated material is able to react with water under practical conditions. Further experiments have to be conducted to explain the effect of lowering the system pressure on water uptake.

References

[1] Visscher, K., Veldhuis, J. B. J., Oonk, H. A. J., van Ekeren, P. J., and Blok, J. G., 2004, "Compacte Chemische Seizoenopslag Van Zonnewarmte; Eindrapportage," ECN Report No. ECN-C-04-074.

[2] Zondag, H. A., Kalbasenka, A., van Essen, V. M., Bleijendaal, L. P. J., Schuitema, R., van Helden, W. G. J., and Krosse, L., 2008, "First Studies in Reactor Concepts for Thermochemical Storage," ECN Report No. ECN-M-9-008.

[3] Brown, M. E., 2001, *Introduction to Thermal Analysis; Techniques and Application*, 2nd ed., Kluwer, Dordrecht, Chap. 3, p. 4.

[4] JCPDS-ICDD, 1997, PDF crystallographic database, JCPDS-ICDD Powder Diffraction File (PDF-2), International Centre for Diffraction Data, Newtown Square, PA.

[5] Seeger, M., Walter, O., Flick, W., Bickelhaupt, F., and Akkerman, O. S., 2007, *Ullmann's Encyclopedia of Industrial Chemistry*, 7th ed., John Wiley and Sons, Inc., electronic release.

[6] Wagman, D. D., Evans, W. H., Parker, V. B., Schumm, R. H., and Halow, I., 1982, "The NBS Tables of Chemical Thermodynamic Properties: Selected Values for Inorganic and C1 and C2 Organic Substances in SI Units," J. Phys. Chem. Ref. Data, **11**, pp. 1–400.

[7] Emons, H. H., Ziegenbalf, G., Naumann, R., and Paulik, F., 1990, "Thermal Decomposition of the Magnesium Sulfate Hydrates Under Quasi-Isothermal and Quasi-Isobaric Conditions," J. Therm. Anal., **36**, pp. 1265–1279.

[8] Ruiz-Agudo, E., Martin-Ramos, J. D., and Rodriguez-Navarro, C., 2007, "Mechanism and Kinetics of Dehydration of Epsomite Crystals Formed in the Presence of Organic Additives," J. Phys. Chem. B, **111**(1), pp. 41–52.

[9] Chipera, S. J., and Vaniman, D. T., 2007, "Experimental Stability of Magnesium Sulfate Hydrates That May Be Present on Mars," Geochim. Cosmochim. Acta, **71**, pp. 241–250.